

Chapter 10.

Detection of Signals in Noise

10.1.Receiver Noise

Noise is the unwanted energy that interferes with the ability of the receiver to detect the wanted signal. It may enter the receiver through the antenna along with the desired signal or it may be generated within the receiver. In underwater sonar systems external acoustic noise is generated by waves and wind on the water surface, by biological agents (fish, prawns etc) and manmade sources such as engine noise. In radar and lidar sensors the external electromagnetic noise is generated by various natural mechanisms such as the sun and lightning amongst others. Manmade sources of electromagnetic noise are myriad, from car ignition systems and fluorescent lights through other broadcast signals.

As discussed earlier, noise within the sensor is generated by the thermal motion of the conduction electrons in the ohmic portions of the receiver input stages. This is known as *Thermal* or *Johnson* Noise.

Noise power P_N is expressed in terms of the temperature T_o of a matched resistor at the input of the receiver

$$P_N = kT_o\beta \text{ W}, \quad (10.1)$$

where: k – Boltzmann’s Constant (1.38×10^{-23} J/K),
 T_o – System Temperature (usually 290K),
 β – Receiver Noise Bandwidth (Hz).

The noise power in practical receivers is always greater than that which can be accounted for by thermal noise alone.

The total noise at the output of the receiver, N , can be considered to be equal to the noise power output from an ideal receiver multiplied by a factor called the Noise Figure, NF

$$N = P_N F_N = kT_o\beta.NF \text{ W}. \quad (10.2)$$

10.2.Noise Probability Density Functions

Consider a typical radar front-end that consists of an antenna followed by a wide band amplifier, a mixer that down converts the signal to an intermediate frequency (IF) where it is further amplified and filtered (bandwidth β_{IF}). This is followed by an envelope detector and further filtering (bandwidth $\beta_V = \beta_{IF}/2$).

The noise entering the IF filter is assumed to be Gaussian (as it is thermal in nature) with a probability density function (PDF) given by

$$p(v) = \frac{1}{\sqrt{2\pi\psi_o}} \exp\left\{-\frac{v^2}{2\psi_o}\right\}, \quad (10.3)$$

where $p(v)dv$ - probability of finding the noise voltage v between v and $v+dv$,
 ψ_o - variance of the noise voltage.

If Gaussian noise is passed through a narrow band filter (one whose bandwidth is small compared to the centre frequency), then the PDF of the post-detection envelope of the noise voltage output can be shown to be

$$p(R) = \frac{R}{\psi_o} \exp\left\{-\frac{R^2}{2\psi_o}\right\}, \quad (10.4)$$

where R is the amplitude of the envelope of the filter output. This has the form of the Rayleigh probability density function

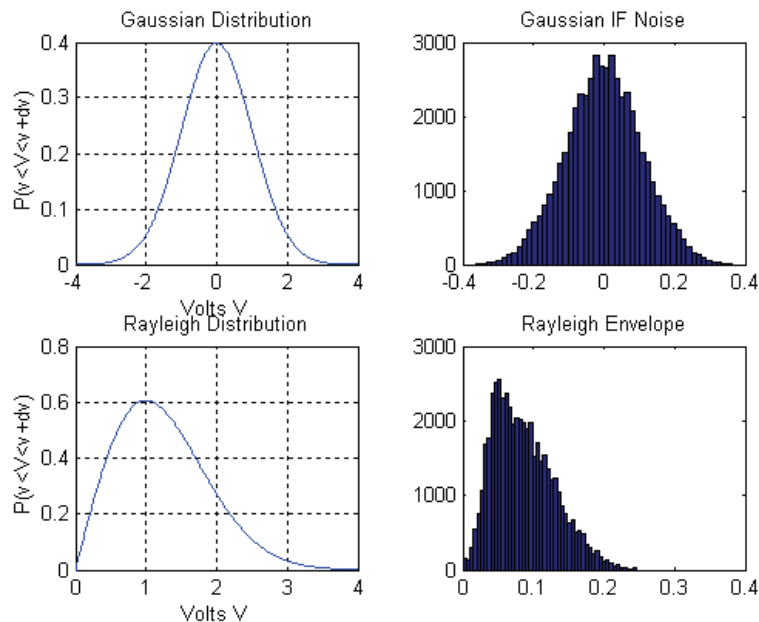


Figure 10.1: Amplitude distributions of thermal noise pre and post detection

10.3. Probability of False Alarm

A false alarm occurs whenever the noise voltage exceeds a defined threshold voltage, V_t , as illustrated in the figure below. The probability of this occurring is determined by integrating the PDF as shown

$$\text{Prob}(V_t < R < \infty) = \int_{V_t}^{\infty} \frac{R}{\psi_o} \exp \frac{-R^2}{2\psi_o} dR = \exp \frac{-V_t^2}{2\psi_o} = P_{fa}. \quad (10.5)$$

It can be seen that the average time interval between crossings of the threshold, called the false alarm time, T_{fa} , can be written as

$$T_{fa} = \lim_{N \rightarrow \infty} \frac{1}{N} \sum_{k=1}^N T_k, \quad (10.6)$$

where T_k – Time between crossings of the threshold V_t by the noise envelope (when the slope of the crossing is positive).

The false alarm probability could also have been defined as the ratio of the time that the envelope is above the threshold to the total time as shown graphically in the figure below

$$P_{fa} = \frac{\sum_{k=1}^N t_k}{\sum_{k=1}^N T_k} = \frac{\langle t_k \rangle_{ave}}{\langle T_k \rangle_{ave}} = \frac{1}{T_{fa} \beta}, \quad (10.7)$$

where t_k and T_k are defined in the figure, and the average duration of a noise pulse is the reciprocal of the bandwidth β .

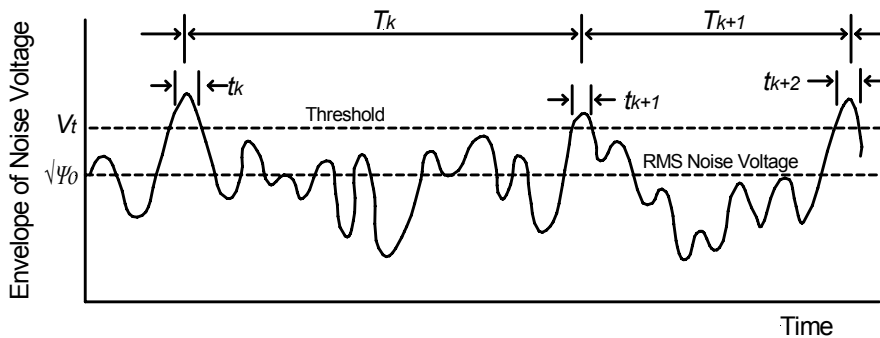


Figure 10.2: Receiver output voltage illustrating false alarms due to noise

For a bandwidth $\beta = \beta_{IF}$, the false alarm time is just

$$T_{fa} = \frac{1}{\beta_{IF}} \exp \frac{V_t^2}{2\psi_o}. \quad (10.8)$$

The false alarm times of practical radars must be very large (usually a couple of hours), so the probability of false alarm must be very small, typically $P_{fa} < 10^{-6}$.

10.4. Probability of Detection

Consider that a sine wave with amplitude, A , is present along with the noise at the input to the IF filter. The frequency of the sine wave is equal to the centre frequency of the IF filter. It is shown by Rice that the signal at the output of the envelope detector will have the following PDF (known as a Rician distribution)

$$p_s(R) = \frac{R}{\psi_o} \exp\left(-\frac{R^2 + A^2}{2\psi_o}\right) I_0\left(\frac{RA}{\psi_o}\right). \quad (10.9)$$

$I_0(Z)$ modified Bessel function of order zero and argument Z . It can be shown that for large Z , an asymptotic expansion for $I_0(Z)$ is

$$I_0(Z) \approx \frac{e^Z}{\sqrt{2\pi Z}} \left(1 + \frac{1}{8Z} + \dots\right). \quad (10.10)$$

The probability that the signal will be detected is the same as the probability that the envelope, R , will exceed the threshold, V_t is

$$p_d = \int_{V_t}^{\infty} p_s(R) dR = \int_{V_t}^{\infty} \frac{R}{\psi_o} \exp\left(-\frac{R^2 + A^2}{2\psi_o}\right) I_0\left(\frac{RA}{\psi_o}\right) dR. \quad (10.11)$$

Unfortunately, this cannot be evaluated in a closed form and so numerical techniques or a series approximation must be used. However, this has already been done, and tables and a series of curves have been produced.

In terms of the PDFs for the noise and the signal plus noise voltages, the detection and false alarm process is shown graphically in the figure below. The lightly shaded area represents the P_{fa} and the dark shaded area (including the tail covered by the light shading) represents the P_d .

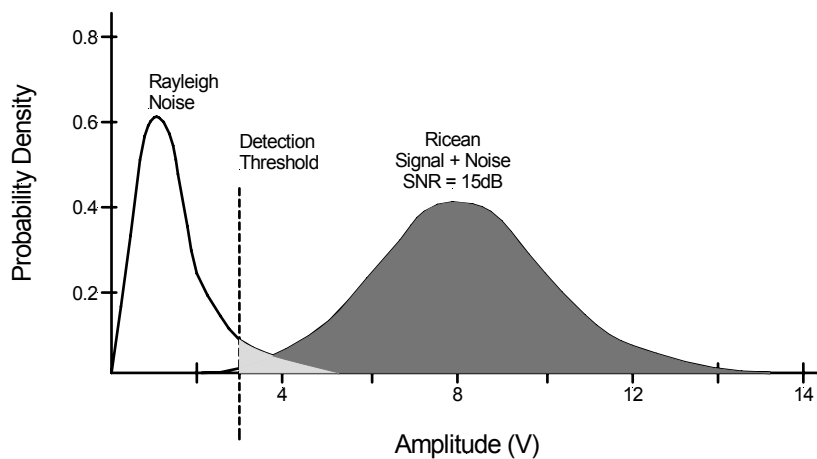


Figure 10.3: PDF's of noise and signal plus noise for $P_{fa} = 10^{-2}$

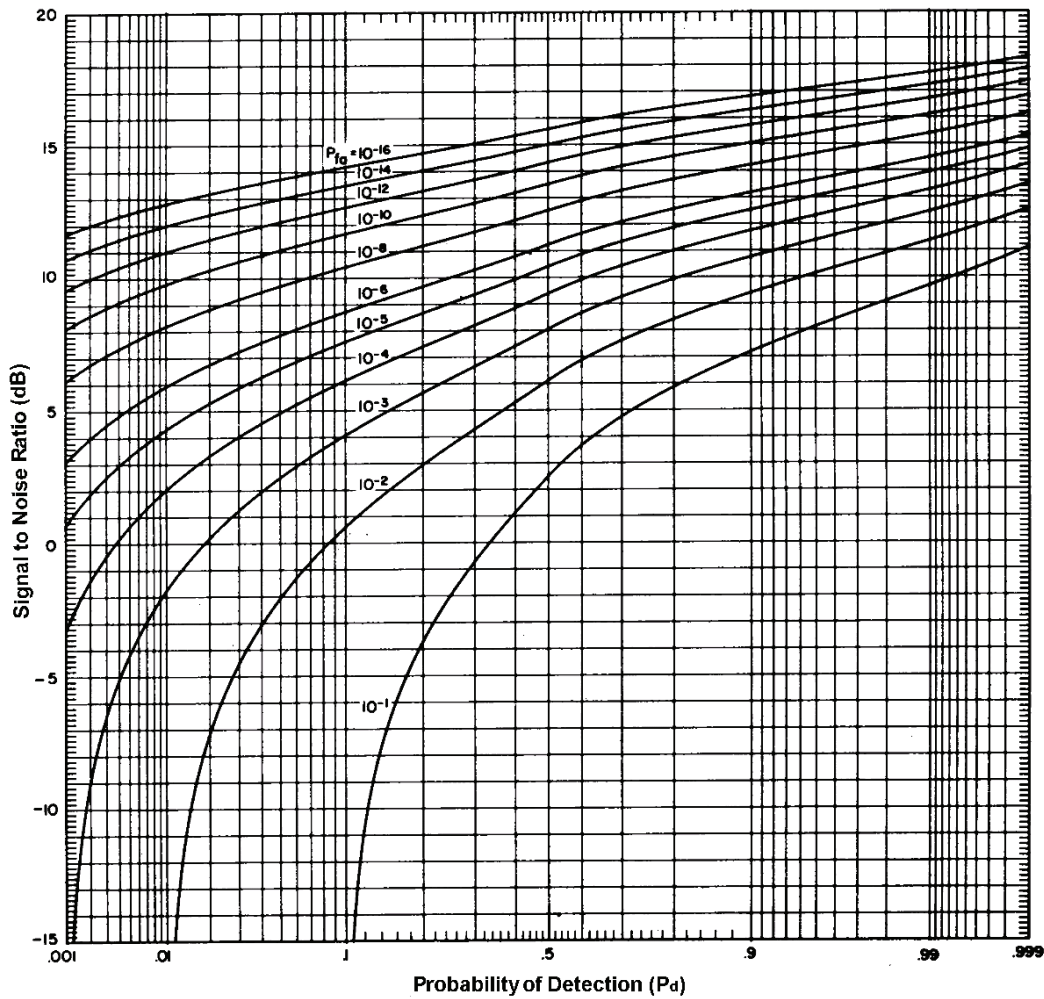


Figure 10.4: Detection probability as a function of signal to noise ratio with false alarm probability as a parameter

A typical radar system will operate with a detection probability of 0.9 and a probability of false alarm of 10^{-6} . The required signal to noise ratio can be read directly off the graph as 13.2dB. Note that this is for a single pulse of a steady sinusoidal signal in Gaussian noise with no detection losses.

```
% Pd and Pfa Determined Numerically by running a time domain simulation
% Generate noise and signals for SNR=13dB
a = (1:1000000);
x = randn(size(a));
sigi = 6.31*sin(a/1000);
y = randn(size(a));
sigq = 6.31*cos(a/1000);
% Determine the envelope
c = sqrt(x.^2+y.^2);
csig = sqrt((x+sigi).*(x+sigi)+(y+sigq).*(y+sigq));
%Plot the distributions
edges=(0:0.1:12);
n=histc(c,edges);
ns=hist(csig,edges);
plot(edges,n,edges,ns);
grid
% Determine the probabilities for different thresholds
vt=5;
% Look for noise peaks above the threshold
nfa = find(c>vt);
```

```

pfa = length(nfa)/1000000
% Look for S+N peaks above the threshold
nd = find(csig>vt);
pd = length(nd)/1000000

```

10.5. Detector Loss Relative to an Ideal System

An envelope detector is used by a radar system when the phase of the received pulse is unknown. This is called non-coherent detection, and it results in a slightly higher SNR requirement than the curves above show.

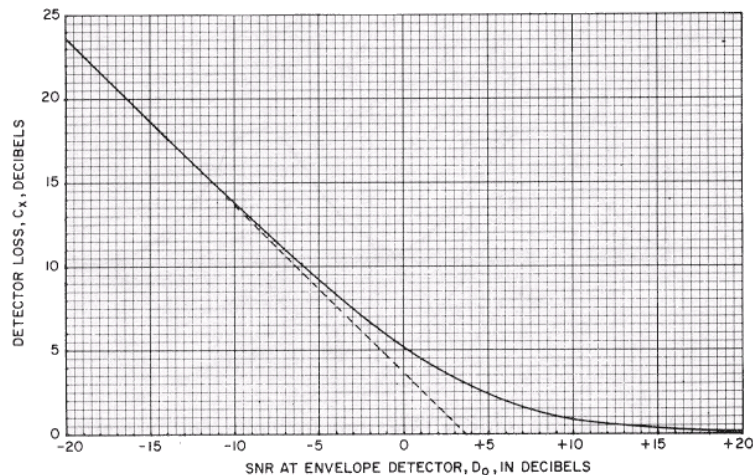


Figure 10.5: Envelope detector loss as a function of signal to noise ratio

This loss factor C_x is approximately

$$C_x(1) \approx \frac{SNR(1) - 2.3}{SNR(1)}, \quad (10.12)$$

where $C_x(1)$ – Loss in SNR,

$SNR(1)$ – The pre detector single pulse SNR required to achieve a particular P_d and P_{fa} .

The graph shows that for good SNR, the detector loss is very small. In the case where the $P_d = 0.9$ and the $P_{fa} = 10^{-6}$ it is only about 0.4dB. This effect is known as small signal suppression as it becomes much more pronounced as the SNR decreases.

One of the advantages of coherent detection is that it has zero response to the quadrature noise component, whereas, this component is translated into phase modulation after envelope detection with the result that the effective SNR in the latter case is degraded. However the phase modulation is very small for high SNR, and few advantages can be gained by coherent detection for $SNR > 10\text{dB}$ ($C_x = 1\text{dB}$) over envelope detection.

10.6. The Matched Filter

To achieve the best possible SNR, the characteristics of the IF filter must be matched to those of the signal pulse.

The peak signal to (average) noise power ratio of the output response of the matched filter is equal to twice the received signal energy, E , divided by the single-sided noise power per Hz, N_o

$$\left(\frac{\hat{S}}{N}\right)_{out} = \frac{2E}{N_o}, \quad (10.13)$$

where \hat{S} – Peak instantaneous signal power seen during the matched filter response to a pulse (W),
 N – Average noise power (W),
 E – Received signal energy (J),
 N_o – Single sided noise power density (W/Hz).

The received energy is the product of the received power, S , as determined by the range equation and the pulse duration, τ

$$E = S\tau, \quad (10.14)$$

And the noise power density is the received noise power, N , divided by the bandwidth, β_{IF}

$$N_o = \frac{N}{\beta_{IF}}. \quad (10.15)$$

Substituting into (10.13)

$$\left(\frac{\hat{S}}{N}\right)_{out} = \frac{2S\tau}{N/\beta_{IF}} = \left(\frac{S}{N}\right)_{in} 2\beta_{IF}\tau. \quad (10.16)$$

When the bandwidth of the signal at IF is small compared to the centre frequency then the peak power is approximately twice the average power in the received pulse. So the output SNR is

$$\left(\frac{S}{N}\right)_{out} \approx \left(\frac{S}{N}\right)_{in} \beta_{IF}\tau. \quad (10.17)$$

The matched filter should not be confused with the circuit theory concept of matching that maximises power transfer rather than SNR.

In practise a matched filter implementation is often hard to achieve exactly, so compromises are made as shown in the following table:

Table 10.1: Efficiency of non-matched filters

| Input Signal Shape | Matched Filter Characteristic | Optimum $B \cdot \tau$ | Loss in SNR compared to Matched Filter (dB) |
|---------------------------|--------------------------------------|--|--|
| Rectangular Pulse | Rectangular | 1.37 | 0.85 |
| Rectangular Pulse | Gaussian | 0.72 | 0.49 |
| Gaussian Pulse | Rectangular | 0.72 | 0.39 |
| Gaussian Pulse | Gaussian | 0.44 | 0 (matched) |
| Rectangular Pulse | Single tuned circuit | 0.4 | 0.88 |
| Rectangular Pulse | Two cascaded tuned circuits | 0.613 | 0.56 |
| Rectangular Pulse | Five cascaded tuned circuits | 0.672 | 0.5 |

10.7. Integration of Pulse Trains

The relationships developed earlier between SNR, P_d and P_{fa} apply to a single pulse only. However, it is possible to improve the radar performance by averaging a number of returns.

For example, as a search-radar beam scans, the target will remain in the beam sufficiently long for more than one pulse to hit it. This number, known as hits per scan, can be calculated as follows

$$n_b = \frac{\theta_b f_p}{\dot{\theta}_s} = \frac{\theta_b f_p}{6\omega_m}, \quad (10.18)$$

where n_b – Hits per scan,
 θ_b – Azimuth beamwidth (deg),
 $\dot{\theta}_s$ - Azimuth scan rate (deg/s),
 ω_m – Azimuth scan rate (rpm).

For a typical ground based radar with an azimuth beamwidth of 1.5° , a scan rate of 5rpm and a pulse repetition frequency of 30Hz, the number of pulses returned from a single point target is 15.

The process of summing all these hits is called integration, and it can be achieved in many ways some of which were discussed in Chapter 5. If integration is performed prior to the envelope detector, it is called *pre-detection* or *coherent* integration, while if integration occurs after the detector, it is called *post-detection* or *non-coherent* integration.

Pre-detection integration requires that the phase of the signal be preserved if the full benefit of the summing process is to be achieved and because phase information is destroyed by the envelope detector, post-detection integration, though easier to achieve, is not as efficient.

If n pulses are perfectly integrated by a coherent integration process, the integrated SNR will be exactly n times that of a single pulse in white noise. However, in the non-coherent case, though the integration process is as efficient, there are the detector

losses discussed earlier that reduce the effective SNR at the output of the envelope detector.

Integration improves the P_d and reduces the P_{fa} by reducing the noise variance and thus narrowing the Noise and Signal + Noise PDFs as shown in the figure below

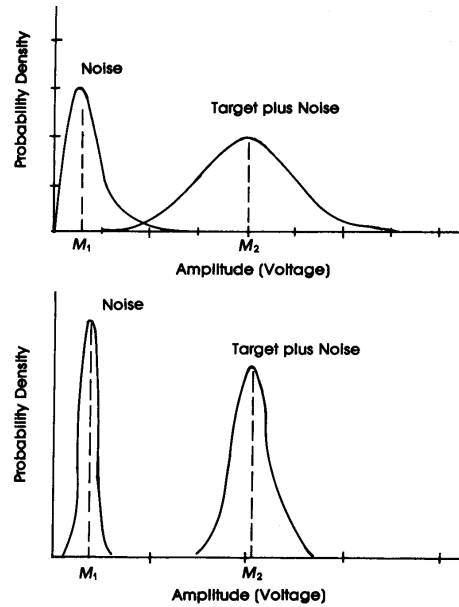


Figure 10.6: Effect of integration on signal and noise PDFs before and after integration

For n pulses integrated, the single pulse SNR required to achieve a given P_d and P_{fa} will be reduced. However, this results in increased detector losses, and hence a reduced effective integration efficiency.

The integration efficiency may be defined as

$$E_i(n) = \frac{SNR(1)}{nSNR(n)}, \quad (10.19)$$

where: $E_i(n)$ – Integration efficiency,

$SNR(1)$ – Single pulse SNR required to produce a specific P_d if there is no integration,

$SNR(n)$ – Single pulse SNR required to produce a specific P_d if n pulses are integrated perfectly.

The improvement in SNR if n pulses are integrated, post detection is thus $nE_i(n)$. This is the integration improvement factor, or the effective number of pulses integrated.

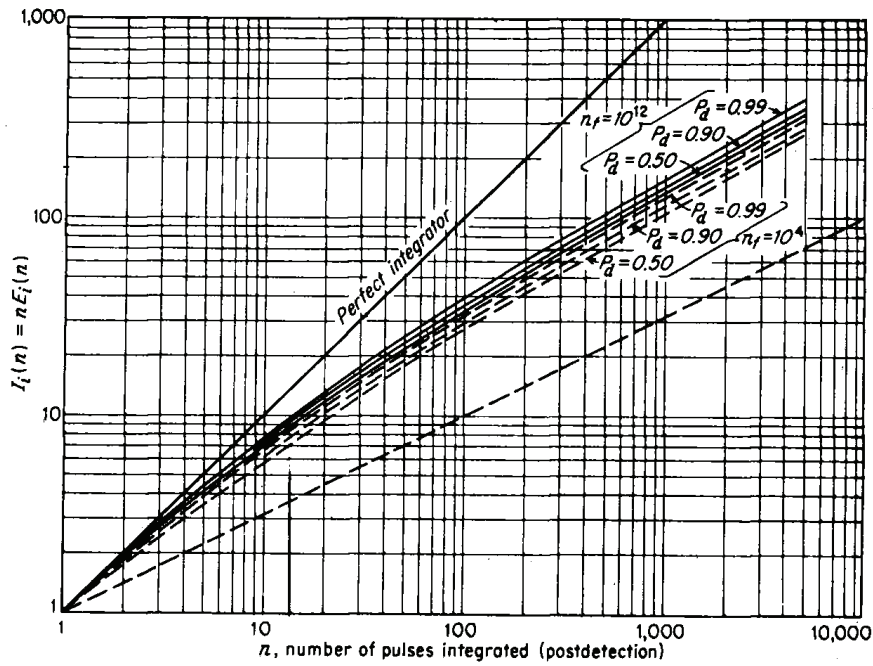


Figure 10.7: Integration improvement factor as a function of pulses integrated

The integration loss in dB is defined as follows

$$L_i(n) = 10 \log_{10} \left(\frac{1}{E_i(n)} \right). \tag{10.20}$$

The integration improvement factor is not a sensitive function of either the P_d or the P_{fa} as can be seen by the clustering of the curves in the figure above.

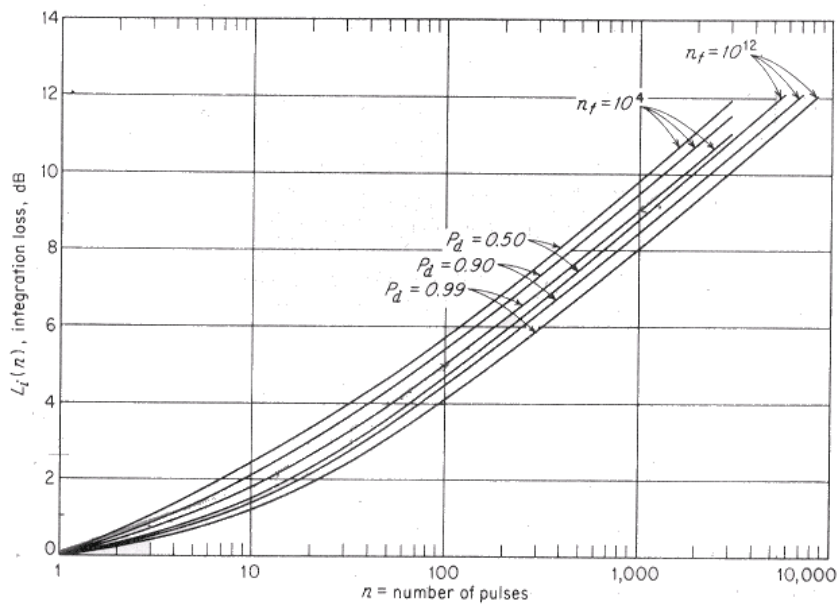


Figure 10.8: Integration loss as a function of the number of pulses integrated

10.8. Detection of Fluctuating Signals

The discussion in the previous section assumes that the signal amplitude does not vary from pulse to pulse during the integration period. However, from the discussion of target cross section in Chapter 9, it is obvious that the RCS of any moving target (with the exception of a sphere) will fluctuate with time as the target aspect as seen by the radar changes.

To properly account for these fluctuations, both the probability density function and the correlation properties with time must be known for a particular target and trajectory. Ideally, these characteristics should be measured for a target, but this is often impractical. An alternative is to postulate a reasonable model for the target fluctuations and to analyse the effects mathematically.

Four fluctuation models proposed by Swerling are used:

- **Swerling 1:** Echo pulses received from the target on any one scan are of constant amplitude throughout the scan, but uncorrelated from scan to scan. The PDF is given by

$$p(\sigma) = \frac{1}{\sigma_{av}} \exp \frac{-\sigma}{\sigma_{av}}, \quad (10.21)$$

where σ_{av} is the average cross section over all target fluctuations.

- **Swerling 2:** The PDF is as for case 1, but the fluctuations are taken to be independent from pulse to pulse.
- **Swerling 3:** The fluctuations are independent from scan to scan, but the PDF is given by

$$p(\sigma) = \frac{4\sigma}{\sigma_{av}^2} \exp \frac{-2\sigma}{\sigma_{av}}. \quad (10.22)$$

- **Swerling:** The PDF is as for case 3, but the fluctuations are independent from pulse to pulse.
- **Swerling 5:** Non fluctuating

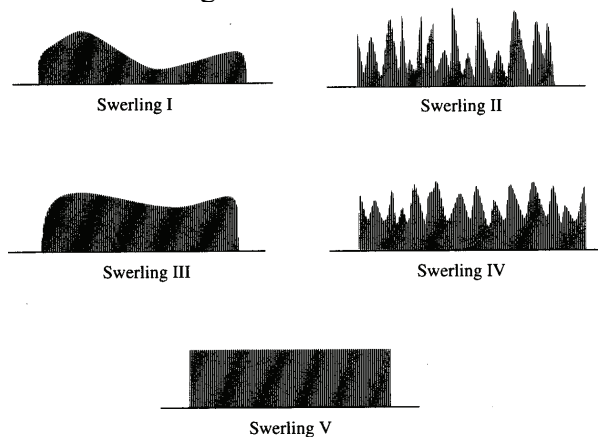


Figure 10.9: Radar returns for different Swerling fluctuations

The PDF for cases 1 and 2 is indicative of a target with many (>5) scatterers of equal amplitude. These are typical for complicated targets like aircraft, while the PDF for cases 3 and 4 is indicative of a target with one large scatterer and many small scatterers.

As one would expect, the single pulse SNR required to achieve a particular P_d (for $P_d > 0.4$) will be higher for a fluctuating target than for a constant amplitude signal. However, for $P_d < 0.4$, the system takes advantage of the fact that a fluctuating target will occasionally present echo signals larger than the average, and so the required SNR is lower.

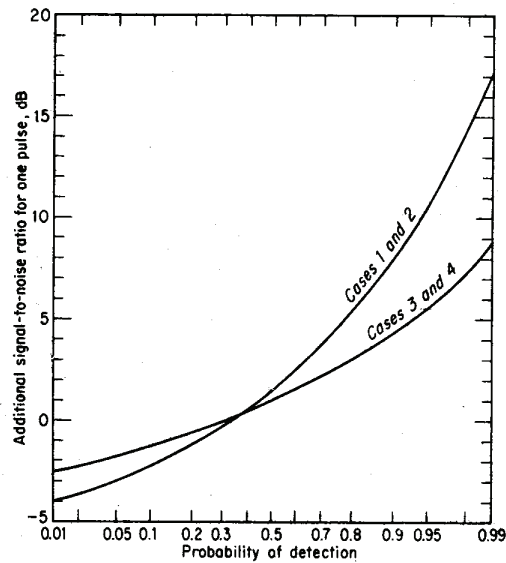


Figure 10.10: Effect of target fluctuation on required signal to noise ratio

To cater for fluctuating targets and integration, a further set of curves describing the integration improvement factor have been developed.

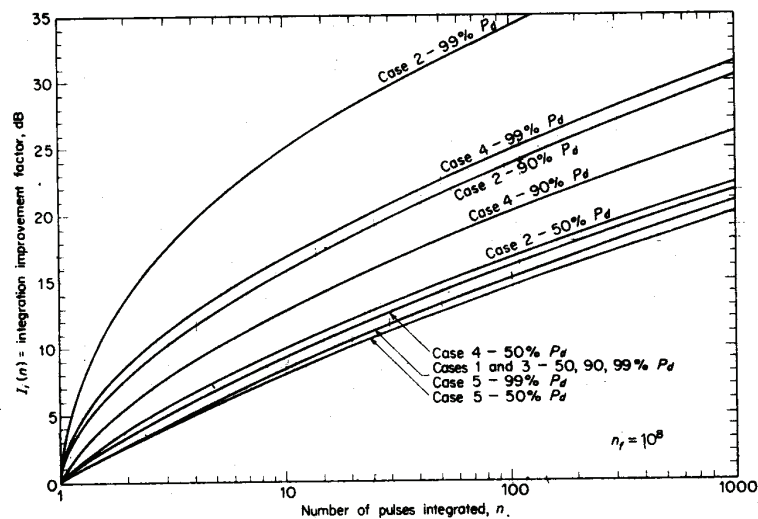


Figure 10.11: Integration improvement factor as a function of the number of pulses integrated for fluctuating targets

If these curves are examined in isolation, it would appear that the integration efficiency $E_I(n) > 1$ under certain conditions. One is not getting something for nothing as the single pulse SNR is much higher in these cases than it would be for the single pulse case.

The procedure for using the range equation when one of these Swerling targets is as follows:

1. Find the SNR for the single pulse, non-fluctuating case that corresponds to the P_d and P_{fa} required using the curves in Figure.10.4
2. For the specific Swerling target, find the additional SNR needed for the required P_d . using the curves in Figure 10.10
3. If n pulses are to be integrated, the integration improvement factor $I_I(n)=nE_I(n)$ is then found using the curves in Figure 10.11
4. The $SNR(n)$ and $nE_I(n)$ are substituted into the range equation along with σ_{av} and the detection range found.

10.9.Constant False Alarm Rate (CFAR) Processors

As can be seen from the tail in the Rayleigh distributed noise power, the false alarm rate is very sensitive to the setting of the detection threshold voltage. Changes in radar characteristics with time (ageing) and changes in the target background characteristics mean that a fixed detection threshold is not practical and so adaptive techniques are required to maintain a constant false alarm rate irrespective of the circumstances. These are called Constant False Alarm Rate (CFAR) processors.

The implementation of CFAR is not difficult, but in general the actual performance will be a function of the target, clutter and noise statistics.

For aircraft these are not a problem as the area around the craft is generally empty so good background statistics can be obtained. However for ground targets, the CFAR threshold is determined from the clutter statistics, which may not be homogeneous. This is made worse by the fact that targets (tanks etc) often hide at the edges of clutter boundaries to reduce the probability of detection.

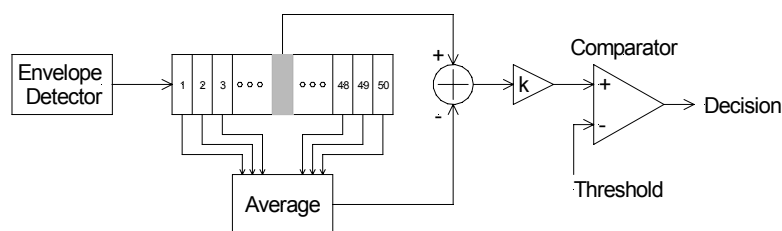


Figure 10.12: Multiple cell averaging CFAR

Needless to say, target detection using the CFAR process introduces additional losses as the statistics are incompletely characterised. For example a cell averaging process will exhibit a 3.5dB loss (compared to an ideal single pulse detector) if 10 cells are used in broadband noise or clutter with a Rayleigh PDF. This decreases to 1.5dB for 20 cells and 0.7dB for 40 cells. The loss decreases with increasing numbers of pulses integrated. For a 10 cell CFAR, with 10 pulses integrated the loss is only 0.7dB and it reduced to only 0.3dB for 100 pulses integrated.

CFAR can operate across range cells, cross-range cells or both, as shown in the figure below.

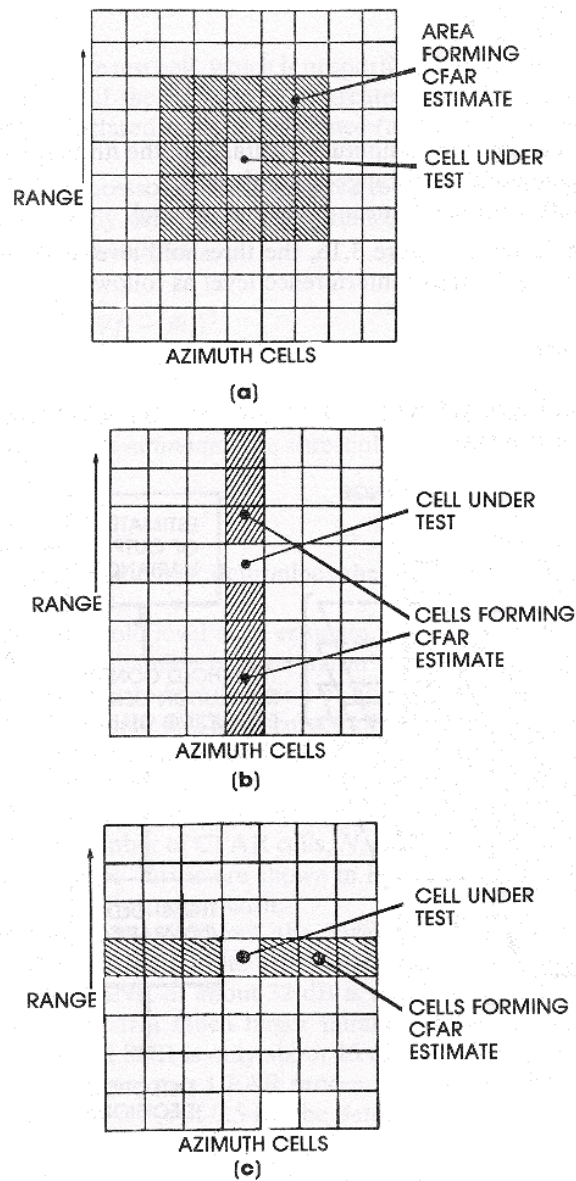


Figure 10.13: Constant false alarm rate options (a) area CFAR, (b) range Only CFAR and (c) azimuth angle only CFAR

In the following examples where a 25+25 point moving average is used to determine the mean value of the signal, it can be seen that the CFAR process detects the two targets without detecting the noise. However, a fixed threshold of 1.8 would perform just as well.

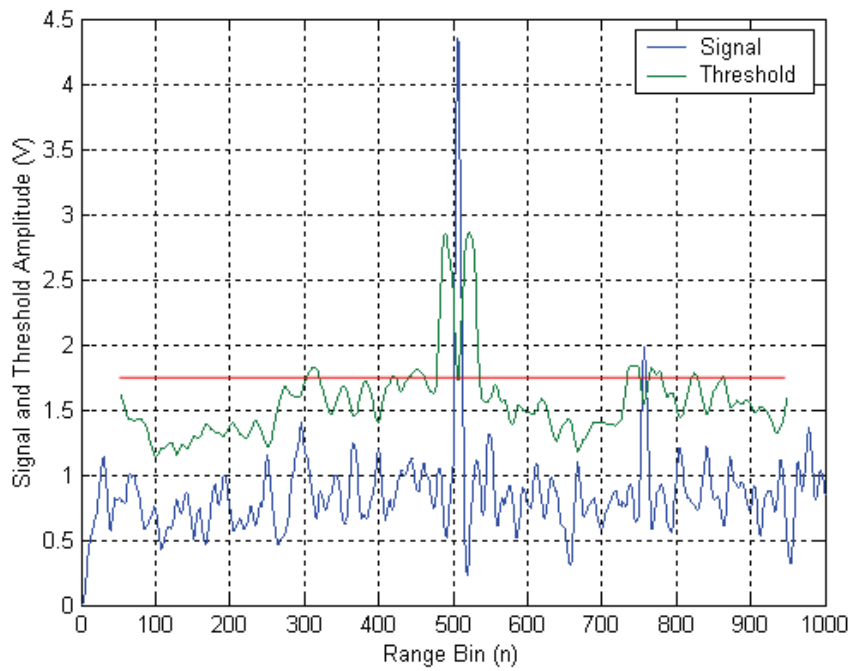


Figure 10.14: CFAR performance for a constant noise floor

In many radar systems, the noise floor varies with range, as shown in the following example. In this instance a fixed threshold does not perform adequately, but the CFAR process still does.

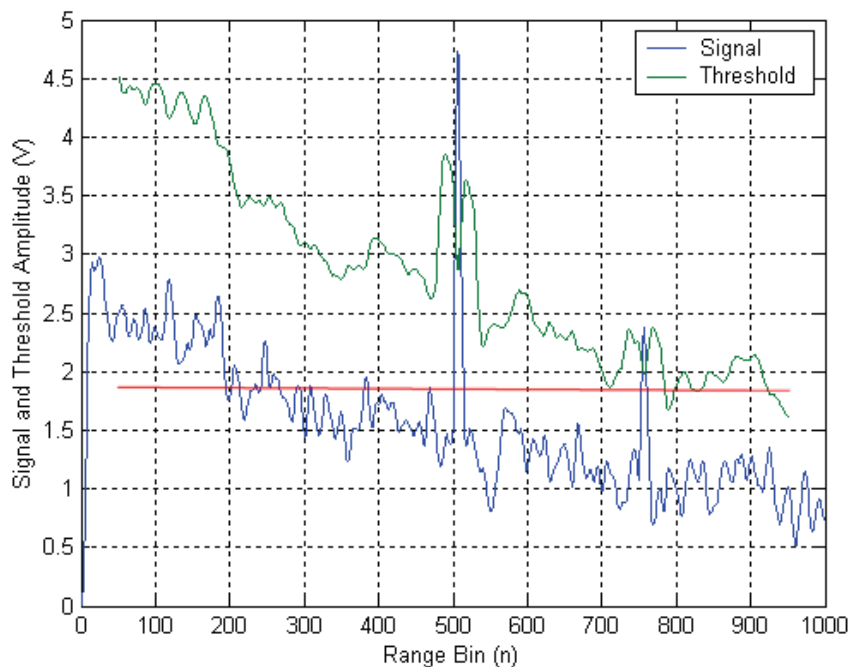


Figure 10.15: CFAR performance for a sloping noise floor

10.10. Air Traffic Control Radar Performance



| | |
|-----------------|--|
| Type: | 2D air surveillance radar |
| Band: | L |
| Frequency: | 1250 to 1350MHz |
| Peak Power: | 5MW |
| Antenna size: | 12.8×6.7m |
| Antenna Gain: | 36dB (lower beam) 34.5dB (upper beam) |
| Beam shape: | Cosec ² |
| Elev beamwidth: | 4° Cosec ² to 40° |
| Azim beamwidth: | 1.25° |
| Scan: | Mechanical |
| Scan Rate: | 6rpm |
| PRF: | 360pps |
| PRF Stagger: | Quadruple |
| Pulse width: | 2μs |
| Noise Figure: | 4dB |

Calculate the theoretical detection range for a 1m² aircraft target if the detection probability $P_d = 0.9$, and the mean time between false alarms is 9 hours.

| | |
|------------------------------------|------------------------------|
| Matched Filter Assumptions: | Rectangular Pulse |
| | Second order bandpass filter |
| | Loss 0.56dB |
| | $B. \tau = 0.613$ |

Hits per Scan: Use the formula $n_b = \frac{\theta_b f_p}{6\sigma_m} = \frac{1.25 \times 360}{6 \times 6} = 12.5$ [use $n_b = 10$]

False Alarm Probability: Use the formula $P_{fa} = \frac{1}{T_{fa}\beta}$

From the matched filter assumptions $B \cdot \tau = 0.613$ and the pulsewidth $\tau = 2\mu\text{s}$, the IF bandwidth $\beta = 306\text{kHz}$.

$$T_{fa} = 9 \text{ hrs} = 32400\text{s}$$

$$P_{fa} = \frac{1}{32.4 \times 10^3 \times 306 \times 10^3} = 10^{-10}$$

Single Pulse SNR: Use the curves in Figure.10.4 for $P_d = 0.9$ and $P_{fa} = 10^{-10}$

$$SNR(1) = 15.2\text{dB}$$

Fluctuating Target: Use the curves in Figure.10.10 for Swerling 2 for an aircraft

Additional SNR required 8dB

Pulse Integration: Use the curves in Figure.10.11 for 10 pulses integrated, a Swerling 2 target and $P_d = 90\%$ to obtain an improvement factor of 15dB

Total n Pulse SNR Required: Add up the requirements

$$SNR(10) = 15.2 + 8 - 15 = 8.2\text{dB}$$

Applying the Radar Range Equation

We assume the following losses:

Transmitter Line = $L_{tx} = 2\text{dB}$ (incorporated into Tx power)

Receiver Line = $L_{rec} = 2\text{dB}$ (incorporated into receiver noise figure)

Losses:

1D Scanning Loss = 1.6dB

Matched Filter = 0.56dB

CFAR Loss = 0.7dB

Misc. Loss = 1.3dB

Total L = 1.6 + 0.56 + 0.7 + 1.3 = 4.16dB

$$P_r = \frac{P_t G^2 \lambda^2 \sigma}{(4\pi)^3 R^4 L}$$

Transmitter Power: $10\log_{10}(5 \times 10^6) = 67\text{dBW}$

Less $L_{tx} = 2\text{dB}$

Radiated peak power $P_t = 65\text{dBW}$

Antenna gain: (Lower beam) 36dB

Radar cross section: $\sigma = 10\log_{10}(1) = 0\text{dBm}^2$

Constant: $10\log_{10} \frac{\lambda^2}{(4\pi)^3} = -45.7\text{dB}$

Received Power: Calculated from the range equation

$$\begin{aligned} P_r &= 65 + 36 + 36 - 45.7 + 0 - 4.16 - 40\log_{10}R \\ &= 87.14 - 40\log_{10}R \quad \text{dBW} \end{aligned}$$

Receiver Noise: Use the equation $N = P_N F_N = kT_{sys} B F_N$

$K = \text{Boltzmann's Constant } 1.38 \times 10^{-23} \text{ J/deg}$

$T_{sys} = \text{Temperature } 290\text{K}$

$B = 306 \times 10^3 \text{ Hz}$

We are given the receiver noise figure in dB

$10\log_{10}(F_n) = 4\text{dB}$

$$N = 10\log_{10}(kT_{sys} B) + 10\log_{10}(F_n) + L_{rec} = -149 + 4 + 2 = -143\text{dBW}$$

Received Signal to Noise Ratio

$$SNR_{rec} = P_r - N = 87.14 - 40\log_{10}R + 143.0 = 230.1 - 40\log_{10}R$$

This must equal the required single pulse SNR if 10 pulses are integrated $SNR(10)$ to achieve the specified P_d and P_{fa} .

$$8.2 = 230.1 - 40\log_{10}R$$

Solving for the Detection Range

Solve for R

$$R = 352.8\text{km}$$

Atmospheric Attenuation

The atmospheric attenuation α_{dB} at L-and is about 0.003dB/km (one way)

So the total two way attenuation over 353km is 2.1dB which will result in a significant reduction of the detection range.

These equations are best solved graphically using MATLAB.

The graph below shows two received power curves, one that does not take into account the atmospheric attenuation which intersects the $SNR(10)$ curve at 353km.

The other graph which takes attenuation into account intersects the $SNR(10)$ curve at 320km.

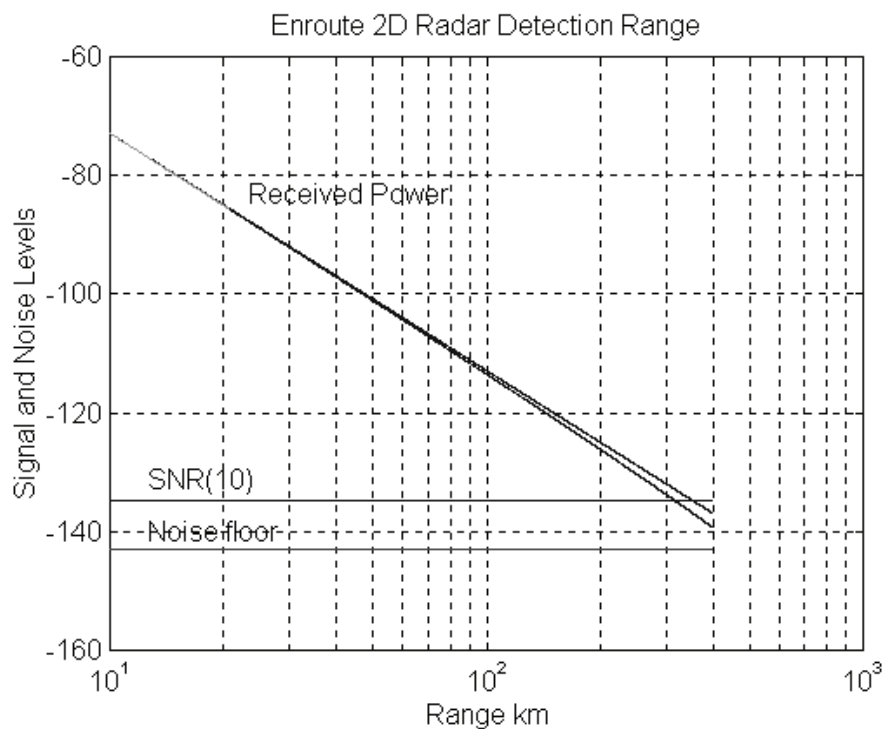


Figure 10.16: Graphical solution to the radar range equation including the atmospheric loss

10.10.1. Analysis Software

Radar performance analysis software based on Blake has been available for many years. In this case a package called RGCALC is used.

For the 2D radar it provides the following results.

```

Radar Name or Description -- Enroute 2D Air Surveillance Radar

Radar and Target Parameters (inputs) --

Peak Pulse Power (kilowatts) ..... 5000.0
Pulse Duration (usec) ..... 2.0000
Transmit Antenna Gain (dB) ..... 36.0
Receive Antenna Gain (dB) ..... 36.0
Frequency (MHz) ..... 1300.0
Receiver Noise Factor (dB) ..... 4.0
Bandwidth Correction Factor (dB) ..... .6
Antenna Ohmic Loss (dB) ..... .0
Transmit Transmission Line Loss (dB) ..... 2.0
Receive Transmission Line Loss (dB) ..... 2.0
Scanning-Antenna Pattern Loss (dB) ..... 1.6
Miscellaneous Loss (dB) ..... 2.0
Number of Pulses Integrated ..... 10
Probability of Detection ..... .900
False-Alarm Probability (Negative Power of Ten) ..... 10.0
Target Cross Section (Square Meters) ..... 1.0000
Target Elevation Angle (Degrees) ..... .40
Average Solar and Galactic Noise Assumed
Pattern-Propagation Factors Assumed = 1

*****

Calculated Quantities (Outputs) --

Noise Temperatures, Degrees Kelvin --
  Antenna (TA) ..... 117.2
  Receiving Transmission Line (TR) ..... 169.6
  Receiver (TE) ..... 438.4
  TE X Line-Loss Factor = TEI ..... 694.9
  System (TA + TR + TEI) ..... 981.7
Two-Way Attenuation Through Entire Troposphere (dB) 3.1

Swerling   Signal-   Tropospheric   Range,   Range,
Fluctuation to-Noise   Attenuation,   Nautical   Kilometers
Case       Ratio, dB   Decibels      Miles

-----
0          6.76      2.77          163.7     303.2
1          15.28     2.13          104.0     192.6
2          7.91       2.70          153.9     285.0
3          11.33     2.45          128.2     237.4
4          7.38       2.73          158.3     293.2

```

Note that the predicted performance using RGCALC for a Swerling 2 target is only 285km, this lower range is because it makes the assumption that the optimum matched filter has $B \cdot \tau = 1$, and hence calculates a wider IF bandwidth by a factor of $1/0.613$ than was made above.

This adds 2.1dB to the noise floor which accounts for the difference

10.11. References

- [1] D.Barton, *Modern Radar Systems Analysis*, Artech, 1988
- [2] M.Skolnik, *Introduction to Radar Systems*, McGraw Hill, 1980
- [3] N.Currie (ed), *Principles and Applications of Millimeter-Wave Radar*, Artech, 1987
- [4] Radar Detection, <http://www.interscience.wiley.com:83/eeee>, 09/03/2001.
- [5] RGCALC Range Analysis Software
- [6] B.Mahafza, *Radar Systems Analysis and Design Using MATLAB*, ChapMan & Hall, 2000